

## ZnO ultraviolet photodiodes with Pd contact electrodes

S.J. Young<sup>a</sup>, L.W. Ji<sup>b</sup>, T.H. Fang<sup>c</sup>, S.J. Chang<sup>a,\*</sup>, Y.K. Su<sup>a</sup>, X.L. Du<sup>d</sup>

<sup>a</sup> Institute of Microelectronics, Department of Electrical Engineering, National Cheng Kung University, Tainan 701, Taiwan

<sup>b</sup> Institute of Electro-Optical and Materials Science, National Formosa University, Yunlin 632, Taiwan

<sup>c</sup> Institute of Mechanical and Electromechanical Engineering, National Formosa University, Yunlin 632, Taiwan

<sup>d</sup> Institute of Physics, Chinese Academy of Sciences, Beijing 100080, China

Received 11 March 2006; received in revised form 29 May 2006; accepted 6 July 2006

Available online 23 October 2006

### Abstract

ZnO epitaxial films were grown on sapphire (0001) substrates by using RF plasma-assisted molecular beam epitaxy (MBE). Metal–semiconductor–metal (MSM) ZnO photodiodes with palladium contact electrodes were then fabricated. With an incident wavelength of 370 nm and an applied bias of 1 V, it was found that maximum responsivity of the Pd/ZnO/Pd MSM photodetectors was 0.051 A W<sup>-1</sup>, which corresponds to a quantum efficiency of 11.4%. Furthermore, it was found that the time constant of our photodiodes was 24 ms with a three-order decay exponential function. For a given bandwidth of 100 Hz and an applied bias of 1 V, we found that noise equivalent power and corresponding detectivity  $D^*$  were  $1.13 \times 10^{-12}$  W and  $6.25 \times 10^{11}$  cm Hz<sup>0.5</sup> W<sup>-1</sup>, respectively.

© 2006 Acta Materialia Inc. Published by Elsevier Ltd. All rights reserved.

**Keywords:** ZnO; Molecular beam epitaxy (MBE); Metal–semiconductor–metal (MSM) photodiodes; Pd

### 1. Introduction

Photodiodes operating in the short-wavelength ultraviolet (UV) region are important devices that can be used in various commercial and military applications. For example, visible-blind UV photodetectors can be used in space communications, ozone layer monitoring, and flame detection. Currently, light detection in the UV spectral range still uses Si-based optical photodetectors. Although these devices are sensitive to visible and infrared radiation, the responsivity in the UV region is low since the room temperature band-gap energy of Si is only 1.2 eV. With the advent of optoelectronic devices fabricated on wide direct band-gap materials, it becomes possible to produce high-performance solid-state photodetectors that are sensitive in the UV region.

Zinc oxide is another wide direct band-gap material that is sensitive in the UV region [1,2]. The large exciton binding energy of 60 meV and the wide band-gap energy of 3.37 eV

at room temperature make ZnO a promising photonic material for applications such as light-emitting diodes (LEDs), laser diodes (LDs), and UV photodetectors. Indeed, ZnO has attracted much attention in recent years [3–5]. High-quality ZnO epitaxial layers can be grown by metalorganic chemical vapor deposition (MOCVD) [1], molecular beam epitaxy (MBE) [6], and pulsed-laser deposition (PLD) [7] on top of ZnO substrates [2], sapphire substrates [8], and epitaxial GaN layers [9].

ZnO Schottky diodes and metal–semiconductor–metal (MSM) photodiodes detecting in the UV region have also been demonstrated [4]. MSM photodiodes consist of interdigitated Schottky contacts deposited on top of an active layer. To produce high-performance MSM UV photodiodes, it is important to achieve a large Schottky barrier height at the metal–semiconductor interface. A large barrier height leads to small leakage current and high breakdown voltage, which could result in improved responsivity and photocurrent to dark current contrast ratio. To achieve a large Schottky barrier height on ZnO, one can choose metals with high-work functions [10]. However, many of the high-work-function metals are not stable

\* Corresponding author. Tel.: +886 6 275 7575x62391; fax: +886 6 2671854.

E-mail address: [changsj@mail.ncku.edu.tw](mailto:changsj@mail.ncku.edu.tw) (S.J. Chang).

at high temperatures. In other words, severe interdiffusion might occur at the metal–ZnO interface. Palladium is an interesting metal that has recently been used as a stable Schottky contact of wide band gap GaN [11–13]. It is a good conductor with superior thermal and chemical stabilities. GaN-based UV PDs and Schottky diodes with Pd contact electrodes have also been demonstrated [13]. Recently, Pd Schottky contacts on ZnO thin films have been investigated [14–16]. Wenckstern et al. studied the lateral homogeneity with an effective barrier height of  $600 \pm 30$  meV and the barrier height of Pd Schottky contacts on ZnO films [14,15]. The Pd–ZnO contacts displayed good rectifying behavior with a high ratio between forward and reverse bias currents at a voltage of  $\pm 1$  V [16]. Wang et al. [17] found the Pd-coated ZnO nanorods has both rapid and easy recoverability for practical applications in hydrogen-selective sensing at ppm levels at room temperature. Although several investigations of ZnO Schottky diodes with Pd contact electrodes have been reported [14,15], we cannot find any studies of the characterization on ZnO-based MSM photodetectors with Pd contacts, such as detectivity.

In this work, we report the growth of ZnO epitaxial layers by MBE and the fabrication of ZnO-based MSM photodetectors with Pd electrodes. Physical properties of the as-grown ZnO epitaxial films and noise behaviors of the fabricated photodetectors will also be discussed.

## 2. Experiments

Samples used in this study were grown by radio frequency (rf) plasma-assisted MBE (Omni Vac) on sapphire (0001) substrates. The base pressure in the growth chamber was  $\sim 1 \times 10^{-10}$  Torr. The source material of Zn was elemental Zn (6 N) evaporated from a commercial Knudsen cell (Crea Tech). Active oxygen and nitrogen radicals were separately produced by two rf-plasma systems (SVTA). The flow rate of oxygen/nitrogen gas was controlled by a mass flow controller (ROD-4, Aera). After being degreased in trichloroethylene and acetone, sapphire substrates were etched in 3:1  $\text{H}_2\text{SO}_4:\text{H}_3\text{PO}_4$  at  $110^\circ\text{C}$  for 30 min followed by rinsing in deionized water. The sapphire substrates were then loaded into the growth chamber. Before growth of the ZnO epilayer, we exposed the sapphire substrates to oxygen radicals for 30 min at  $180^\circ\text{C}$  with 350 W rf power and 2.5 sccm oxygen flux in order to form an O-terminated sapphire surface. After this oxygen radical pre-growth treatment, we performed nitridation at  $180^\circ\text{C}$  for 1 h with 480 W rf power and 3.0 sccm nitrogen flux. It should be noted that the formation of a uniform O-terminated surface before nitridation is crucial for the formation of N-polar AlN and suppression of the Zn-polar inversion domains (the Zn-polar domains in an O-polar ZnO matrix, for instance) to achieve uniform O-polar ZnO films. Besides, the nitridation involves the diffusion of nitrogen atoms into sapphire and substitution for oxygen, and an N-polar AlN thin layer is formed as a result

of the atom substitution. From the reflection high-energy electron diffraction patterns, a very thin AlN layer ( $\sim 2$  nm) will be formed with a  $30^\circ$  in-plane rotation of its lattice with respect to that of the sapphire substrate [18]. After nitridation, we grew a 1000-nm-thick unintentionally doped ZnO epitaxial layer using a conventional two-step growth method, i.e., a low-temperature buffer layer growth at  $400^\circ\text{C}$  and a high-temperature growth at  $650^\circ\text{C}$ . The ZnO epitaxial layer was annealed at  $750^\circ\text{C}$ . At this moment, we could observe a  $3 \times 3$  reconstruction pattern, which indicates the O-polar nature of the ZnO films [19]. Therefore, oxygen plasma pretreatment before surface nitridation was introduced and applied to obtain unipolar single-domain ZnO films of high quality. It was found by Hall measurement that the carrier concentration of the as-grown ZnO films was  $1.71 \times 10^{16} \text{ cm}^{-3}$  at room temperature. The samples were then characterized by photoluminescence (PL) and X-ray diffraction (XRD).

ZnO MSM photodetectors were then fabricated. Prior to the deposition of contact electrodes, wafers were dipped in acetone and methanol to clean the surface. A 100-nm-thick Pd film was subsequently deposited onto the sample surface by e-gun evaporation to serve as the metal contact. Standard lithography and etching were then performed to define the interdigitated contact pattern. The fingers of the Pd contact electrodes were  $13 \mu\text{m}$  wide and  $146 \mu\text{m}$  long, with  $8 \mu\text{m}$  spacing. The active area of the whole device was  $146 \times 146 \mu\text{m}^2$ . The photocurrent and dark current of the fabricated photodetectors were then measured by an HP4145B semiconductor parameter analyzer. Spectral responsivity measurements were also performed using a light source (Oriel Optical System) which employed a 250 W xenon arc lamp and a monochromator covering the range 300–600 nm. Low-frequency noises of the fabricated photodetectors were also measured in the frequency range of 1–100 kHz using a low-noise current preamplifier and an HP35670A fast Fourier transform (FFT) spectrum analyzer.

## 3. Results and discussion

Fig. 1 shows the room temperature PL spectrum of these ZnO epitaxial films. We observed a strong excitonic related PL peak at 3.31 eV (375 nm) and a very weak green band emission at around 2.77 eV. The green luminescence band may be due to the oxygen vacancy as the defect. It was also found that full-width half-maximum (FWHM) of the excitonic related PL peak was only 106 meV [8]. Furthermore, it was found that the intensity ratio between the excitonic band and the green band emission was extremely large and no deep level broadband luminescence was observed. These results all indicate good crystal quality of our ZnO epitaxial layers [8]. The inset of Fig. 1 shows the measured XRD spectrum of the 1000-nm-thick ZnO epitaxial film prepared on sapphire substrate. The peak occurring at  $2\theta = 41.9^\circ$  in the spectrum originated from the (006) plane of the sapphire substrate. We also observed a ZnO (002)

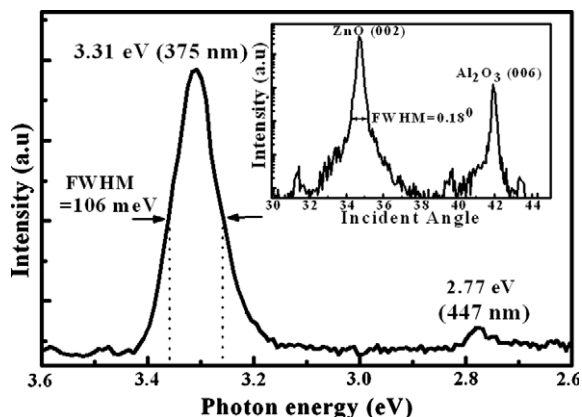


Fig. 1. Room temperature PL spectrum of epitaxial ZnO films. The inset shows XRD spectrum of the epitaxial ZnO films prepared on sapphire substrate.

XRD peak at  $2\theta = 34.3^\circ$  with a FWHM of  $0.18^\circ$ . Such a result indicates that the ZnO film was preferentially grown in the  $c$ -axis direction. The small FWHM of the ZnO (002) XRD peak again indicates the good crystal quality of our samples.

Fig. 2 shows the current–voltage ( $I$ – $V$ ) characteristics of the fabricated ZnO MSM photodetectors with Pd electrodes measured in the dark and under illumination (370 nm) with an optical power of  $100 \text{ mW m}^{-2}$ . Using thermionic emission theory and the dark current measured in Fig. 2, we found that the Schottky barrier height at the Pd/ZnO interface was around 0.701 eV. It was also found that the dark current and photocurrent of the fabricated photodiode biased at 1 V were  $1.19 \times 10^{-8}$  and  $3.83 \times 10^{-6}$  A, respectively. In other words, we achieved a photocurrent to dark current contrast ratio of only 322. We should be able to significantly improve this contrast ratio by annealing the Pd electrodes [11–13]. Previously, it has been shown that one can achieve a higher barrier height by annealing the Pd contacts on GaN. It is known that

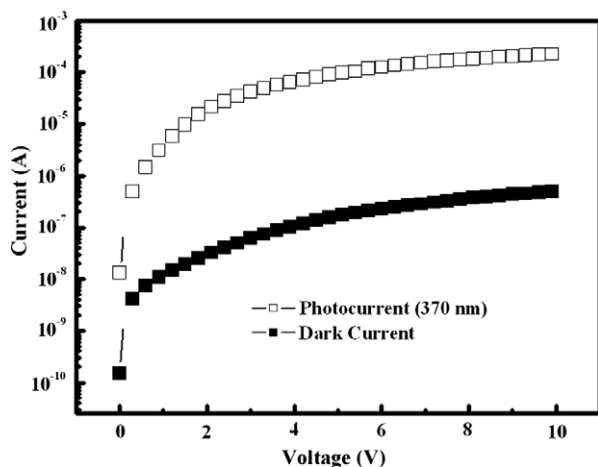


Fig. 2.  $I$ – $V$  characteristics of the fabricated Pd/ZnO/Pd MSM photodiodes measured in the dark (dark current) and under 370 nm illumination (photocurrent).

the annealing process can produce good electrical conductivity and a high work function ( $>5.0$  eV). We believe that the annealing process should also form good Schottky contacts on our  $n$ -ZnO epitaxial layers so that we should be able to effectively suppress the dark current. Thus, we can achieve a much larger photocurrent to dark current contrast ratio after annealing. Such experimentation is underway and the results will be reported separately.

Fig. 3 shows measured spectral responsivities of the fabricated Pd/ZnO/Pd MSM photodetectors. As shown in the figure, it was found that the photodetector responsivities were nearly constant in the below band gap UV region (300–370 nm), while sharp cutoffs with a drop of two orders of magnitude occurred at approximately 370 nm. With an incident wavelength of 370 nm and 1 V applied bias, it was found that the maximum responsivities for the fabricated Pd/ZnO/Pd MSM photodetectors was  $0.051 \text{ A W}^{-1}$ , which corresponds to a quantum efficiency (QE) of 11.4%.

Fig. 4 shows the transient response in current of the fabricated ZnO MSM photodetectors when the lamp was removed. It was found that photocurrent decayed rapidly and could be well-described by the stretched-exponential function. Using the three-order exponential fit to our experimental data, we found that the time constant  $\tau = 24$  ms. This value indicates that the response speed of these ZnO MSM UV photodetectors is faster than those measured from ZnSe-based photodetectors with similar structures [20,21]. It also suggests that ZnO MSM photodetectors are potentially useful in the UV-spectral region.

In this paper, we calculated the detectivity ( $D^*$ ) and noise equivalent power (NEP) of the fabricated ZnO MSM photodetectors as compared with the other compound semiconductor devices. The low-frequency noise spectra was then measured. Fig. 5 shows the low-frequency noise spectra of the ZnO MSM photodetectors with Pd electrodes. From these curves, it was found that measured noise power densities,  $S_n(f)$ , could be fitted well by  $1/f^2$  with

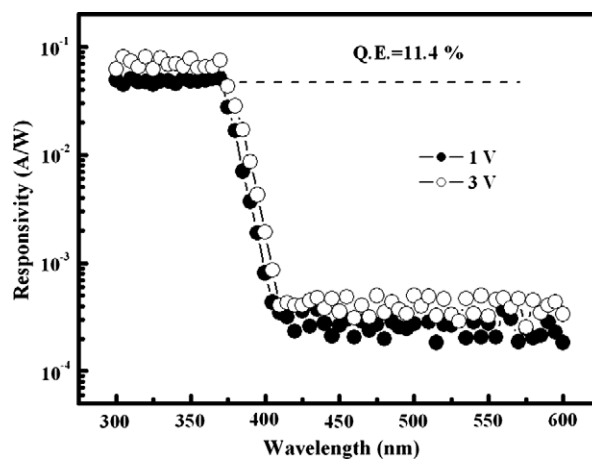


Fig. 3. Measured spectral responsivities of the fabricated Pd/ZnO/Pd MSM photodiodes.

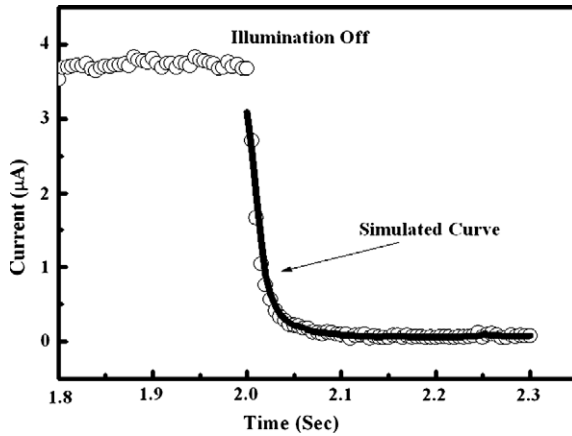


Fig. 4. Transient response in current of the fabricated ZnO MSM photodiodes when the lamp was removed.

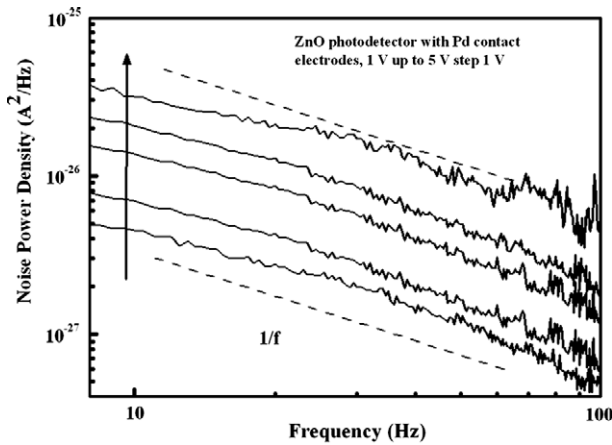


Fig. 5. Low-frequency noise spectra of the Pd/ZnO/Pd MSM photodiodes.

$\gamma = 1$ . The observed pure  $1/f$  noise indicates that trapping states are distributed uniformly in energy between the ZnO and Pd electrodes. For a given bandwidth of  $B$ , we could estimate the total square noise current by integrating  $S_n(f)$  over the frequency range.

$$\begin{aligned} \langle i_n \rangle^2 &= \int_0^B S_n(f) df = \int_0^1 S_n(1) df + \int_1^B S_n(f) df \\ &= S_0 [\ln(B) + 1] \end{aligned} \quad (1)$$

Here, we assumed  $S_n(f) = S_n(1 \text{ Hz})$  for  $f < 1 \text{ Hz}$ . Thus, the noise equivalent power (NEP) can be given by:

$$\text{NEP} = \frac{\sqrt{\langle i_n \rangle^2}}{R} \quad (2)$$

where  $R$  is the responsivity of the photodetectors. The normalized detectivity  $D^*$ , could then be determined by:

$$D^* = \frac{\sqrt{A}\sqrt{B}}{\text{NEP}} \quad (3)$$

where  $A$  and  $B$  are the area of the photodetector and the bandwidth, respectively. For a given bandwidth of

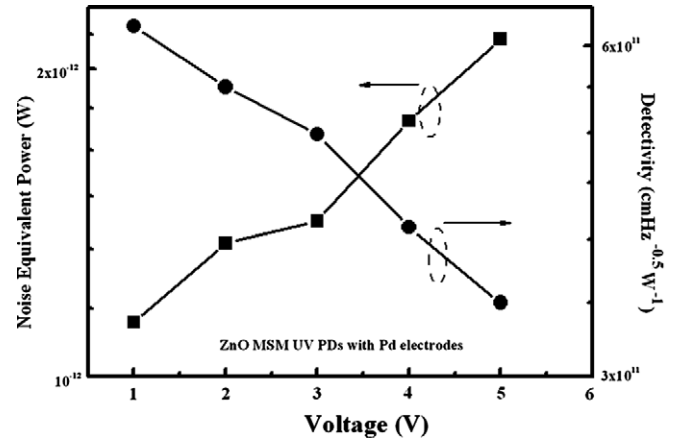


Fig. 6. The noise equivalent power and detectivity as functions of applied voltage.

100 Hz and an applied bias of 1 V, we found that NEP and corresponding detectivity of these Pd/ZnO/Pd MSM photodetectors were  $1.13 \times 10^{-12} \text{ W}$  and  $6.25 \times 10^{11} \text{ cm Hz}^{0.5} \text{ W}^{-1}$ , respectively. It should be noted that the value of  $D^*$  measured from the fabricated photodetectors were higher than that observed from the GaN-based and ZnSe MSM photodetectors [22,23]. Such a result can be attributed to the high crystal quality of the as-grown ZnO epitaxial films with very low-defect density. In addition, the good interface between Pd and ZnO also results in small noise.

It was also found that the measured noise power densities could be fitted well by the following equation:

$$S_n(f) = K \left( \frac{I_d^\beta}{f^\gamma} \right) \quad (4)$$

where  $S_n(f)$  is the spectral density of the noise power,  $K$  is a constant,  $I_d$  is the dark current, and  $\beta$  and  $\gamma$  are two fitting parameters. It was found that  $\beta$  and  $\gamma$  were 1.8 and 1, respectively. Such a result agrees well with Kleinpenning's model that the spectral density of  $1/f$  noise should be proportional to  $I_d^2$  [24].

Fig. 6 shows that the NEP increased and  $D^*$  decreased monotonically with the applied bias. This is due to the fact that the increase in responsivity is much smaller than the increase of total noise current power as the applied bias increased for our detectors. Thus, the NEP and  $D^*$  of our detectors were both dominated by the total noise current power.

#### 4. Conclusion

In summary, ZnO epitaxial films were grown on sapphire substrates by MBE. Pd/ZnO/Pd MSM UV photodetectors were also fabricated. It was found that barrier heights for electrons were 0.701 eV. With an incident wavelength of 370 nm and applied bias of 1 V, it was found that the responsivity for the photodetectors was  $0.051 \text{ A W}^{-1}$ , which corresponds to a quantum efficiency of 11.4%. Fur-

thermore, it was also found that NEP and corresponding detectivity of the Pd/ZnO/Pd MSM photodetectors were  $1.13 \times 10^{-12} \text{ W}$  and  $6.25 \times 10^{11} \text{ cm Hz}^{0.5} \text{ W}^{-1}$ , respectively.

### Acknowledgement

This work was supported by National Science Council under NSC 94-2215-E-150-009.

### References

- [1] Barnes TM, Leaf J, Hand S, Fry C, Wolden CA. *J Appl Phys* 2004;96:7036.
- [2] Kato H, Sano M, Miyanoto K, Yao T. *Jpn J Appl Phys* 2003;42:L1002.
- [3] Lee W, Jeong MC, Myoung JM. *Acta Mater* 2004;52:3949.
- [4] Liang S, Sheng H, Liu Y, Huo Z, Lu Y, Shen H. *J Cryst Growth* 2001;225:110.
- [5] Mang A, Reimann K, Rübenacke St. *Solid State Commun* 1995;94:251.
- [6] Setiawan A, Vashaei Z, Cho MW, Yao T, Kato H, Sano M, et al. *J Appl Phys* 2004;96:3763.
- [7] Kaidashev EM, Lorenz M, von Wenckstern H, Rahm A, Semmelhack HC, Han KH, et al. *Appl Phys Lett* 2003;82:3901.
- [8] Sakurai K, Iwata D, Fujita S, Fujita S. *Jpn J Appl Phys* 1999;38:2606.
- [9] Ko HJ, Chen YF, Hong SK, Yao T. *J Cryst Growth* 2000;209:816.
- [10] Auret FD, Goodman SA, Hayes M, Legodi MJ, van Laarhoven HA, Look DC. *Appl Phys Lett* 2001;79:3074.
- [11] Duxstad KJ, Haller EE, Yu KM. *J Appl Phys* 1997;81:3134.
- [12] Kim CC, Je JH, Kim DW, Baik HK, Lee SM, Ruterana P. *Mater Sci Eng B* 2001;82:105.
- [13] Schmitz AC, Ping AT, AsifKhan M, Chen Q, Yang JW, Adesida I. *Electron Lett* 1996;32:1832.
- [14] von Wenckstern H, Kaidashev EM, Lorenz M, Hochmuth H, Biehne G, Lenzner J, et al. *Appl Phys Lett* 2004;84:79.
- [15] von Wenckstern H, Biehne G, Rahman RA, Hochmuth H, Lorenz M, Grundmann M. *Appl Phys Lett* 2006;88:092102.
- [16] Grossner U, Gabrielsen S, Borseth MB, Grillenberger J, Kuznetsov AY, Svensson G. *Appl Phys Lett* 2004;85:2259.
- [17] Wang HT, Kang BS, Ren F, Tien LC, Sadik PW, Norton DP, et al. *Appl Phys Lett* 2005;86:243503.
- [18] Mei ZX, Wang Y, Du XL, Ying MJ, Zeng ZQ, Zheng H, et al. *J Appl Phys* 2004;96:7108.
- [19] Chen YF, Ko HJ, Hong SK, Yao T. *Appl Phys Lett* 2000;76:559.
- [20] Seghier D, Gislason HP. *J Cryst Growth* 2000;214:511.
- [21] Hu GJ, Zhang L, Dai LN, Chen LY, Tamargo MC. *Solid State Commun* 1999;111:631.
- [22] Wang CK, Chang SJ, Su YK, Chiou YZ, Chang CS, Lin TK, et al. *Semicond Sci Tech* 2005;20:485.
- [23] Vigué F, Tournié E, Faurie JP. *IEEE J Quan Electron* 2001;37:1146.
- [24] Kleinpenning TGM. *Solid State Electron* 1979;22:121.